THE SOURCE OF EMITTANCE DILUTION AND PHOTOEMISSION TUNNELING EFFECT IN PHOTOCATHODE RF GUNS*

V. Volkov, BINP SB RAS, Novosibirsk, Russia
R. Barday, T. Kamps, J. Knobloch, A. Matveenko, S. Schubert, J. Voelker, HZB, Berlin, Germany,
J. Sekutowicz, DESY, Hamburg, Germany

Abstract

Experimental data on HoBiCaT SRF photoinjector give an emittance which is much larger than the predicted for the idealized setup. Modeling of photocathode RF gun beams with the different imperfections of experimental setup (alignment errors, inhomogeneity of quantum efficiency and laser power distributions on the cathode) is given. The main reason for the beam emittance dilution is photocathode field imperfections induced by field emitters that change the local electric field. Some field models of such photocathodes are tested in the simulations.

The dependence of photocathode beam currents on the surface electric field was measured with the HoBiCaT SRF Photoinjector. The dependence can be explained by the tunneling effect described by Fowler-Nordheim like equation and is difficult to explain with the Schottky effect.

INTRODUCTION

At the end of 2011 the beam experiments with a superconducting 1.3 GHz SRF gun with a deposited Pb photocathode were carried out at HZB [1]. Some beam parameters are discussed in the paper.

The experimental test stand is presented in Fig.1. Main parameters of the experimental setup are listed in Fig. 1.

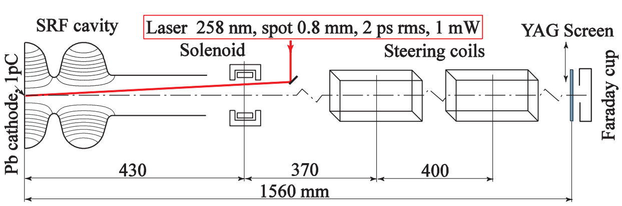

Figure 1: A sketch of the experimental setup.

The lead photocathode is deposited on the back wall of the cavity on the axis. The emitted electrons from the photocathode propagate through the beam pipe of the cavity, the SC solenoid, and two steering coils. The bunch is visualized on the screen or dumped in the Faraday cup. Two types of data are considered: the image of the beam on the screen for emittance measurements, and the Faraday cup measurements of the current vs. the cavity field.

EMITTANCE MEASUREMENTS

The beam in the experiments has relatively small size due to the small laser spot and short pulse width. Also it has a low bunch charge (see Table 1). These are the reasons for negligible dilution of the bunch emittance by time dependent RF gun field, its nonlinearities, and space charge forces [2], i.e. the beam must save the initial photocathode emittance (thermal emittance).

Analytically calculated [3] thermal normalized rms emittance is 0.212 µm. But the measurement shows that emittance is a magnitude more than the predicted. The sources of the emittance dilution are analyzed in this paper by numerical dynamics simulation.

The beam emittance was measured by the solenoid scan method [4] where the transversal bunch size ($\sigma_{x,y}$) of the beam vs. the solenoid field was measured. This size depends also on the particle energy (*E*) that is changed by the launch phase scanning at different cavity fields. The experimental results are shown in Fig.2.

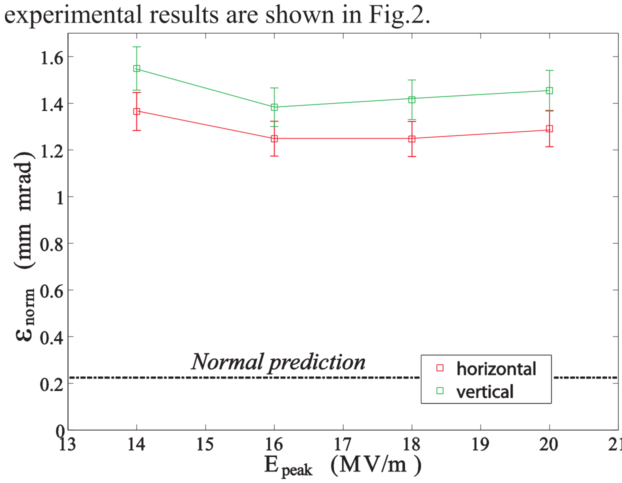

Figure 2: Normalized Emittans vs cathode field with the launch phase of 25º.

Analysis of the Emittance Dilution Sources

In Table 1 the influence of these imperfections except surface cathode field imperfections are listed.

Table 1: Emittance dilution by setup imperfections

Parameter	**Imperfection**	**Dilution**
Laser width	σ_z=2→5 ps	3.5%
Density uniformity	-50% / +50%	5%
Space charge	q=0→1 pC	11%
Steer coil offset	Y_{offset}=3 mm	18%
Solenoid offset	Y_{offset}=3 mm	18.4%
Cathode offset	Y_{offset}=3 mm	97%

* Work supported by Bundesministerium fuer Bildung und Forschung, Land Berlin, and grants of Helmholtz Assiciation VH-NG-636 and HRJRG-214.

Copyright © 2012 by IEEE – cc Creative Commons Attribution 3.0 (CC BY 3.0) — cc Creative Commons Attribution 3.0 (CC BY 3.0)

The analyzed imperfections in the setup are following: space charge forces of 1 pC bunch charge, laser pulse width, uniformity of the laser transverse distribution (3 times increased density from the lower edge of the spot to the upper one), cathode offset from the cavity, steer coil offset (their 3D magnetic field map was used for ASTRA simulation), solenoid offset, and surface cathode field imperfections. As a rule the imperfection influence (except the cathode offset and cathode surface imperfections) is of the order of the measuring accuracy.

Cathode Field Imperfections

We consider the cathode field imperfections are produced by the surface micro profile (emitters) such as those shown in Fig.3. In the simulation two types of ellipsoidal like emitters are used: knobs with the diameter of *2* μm having the field enhancement factor of $\beta=5.4$, and blobs with the diameter of *200* μm and $\beta=2, 4.2$.

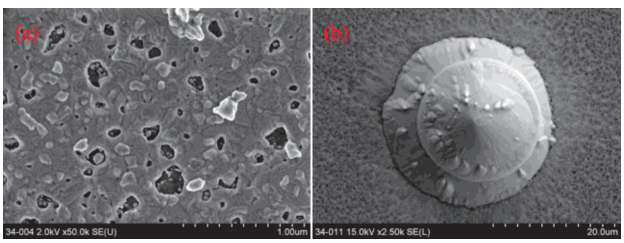

Figure 3: SEM picture of Lead deposited on niobium substrate. (a) 1 μm scale (“Knobs”), (b) 20 μm scale (“Blob”).

In the ASTRA simulation the 3D field map of these emitters randomly scattered on the cathode surface is used. The field distribution of them is presented in Fig.4. Such a field imperfection has significant influence on the particle dynamics and beam emittance dilution that reaches 850% (see Table 2) if compare with the thermal one (0.212 μm).

Table 2: Beam characteristics with different field imperfections on the cathode

	E_{max}, MV/m	$\varepsilon_x/\varepsilon_y$, μm	σ_x/σ_y, μm
1 blobs (β=4.2)	20	1.20	88
3 blobs (β=2)	20	1.07/1.13	122/134
7 Knobs(β=5.4)	20	0.349	61/60.1
14 knobs(β=5.4	20	0.427	72.4/69.7
3 blobs (β=2) + 14 knobs (β=5.4) (see Fig.4)	20	1.41/1.42	98.9/112
	18	1.46/1.43	113/115
	16	1.54/1.45	136/143
	14	1.66/1.50	171/174
	12	1.81/1.59	230/228

In Figs. 5, 6 transversal particle distributions of the emitted bunch at 2 mm far from the photocathode are shown. In the experiment the screen image like Figs. 5a, 5b is observed (see Fig.6).

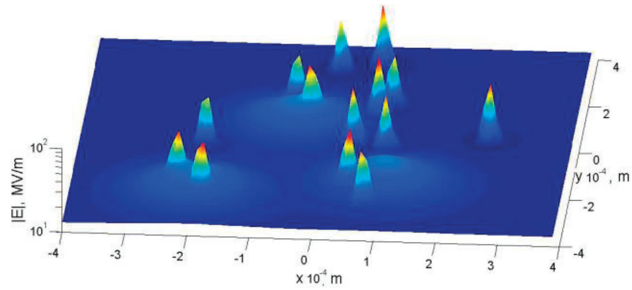

Figure 4: 3D map of the cathode field distribution with 3 blobs and 14 knobs randomly scattered on the cathode.

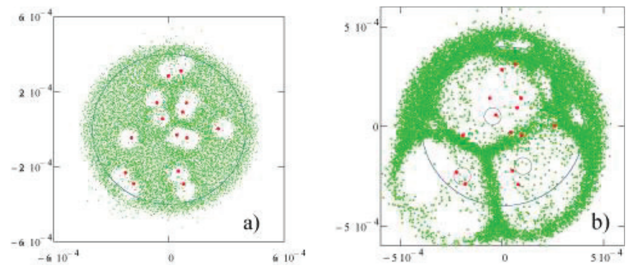

Figure 5: Bunch particle (green) distribution at 2 mm from the cathode. The blue cycle is the cathode boundary. a) 14 knobs on the cathode surface in red. b) The same 14 knobs on the surface and 3 blobs (see Fig.4).

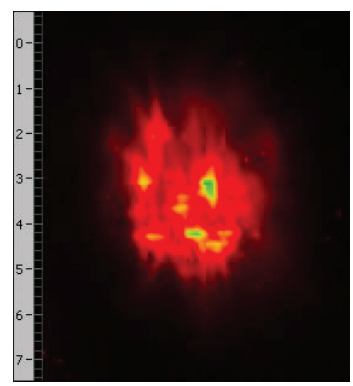

Figure 6: Beam screen image. (mm scale).

PHOTOCURRENT

The laser pulse driven photo current depends on the cathode surface electric field density (E_{surf}). Schottky theory [5] predicts $I= I_0 +(A_s+B_s\cdot E_{surf}^{1/2})^2$, where A_s and B_s are coefficients usually found by fitting of experimental data with $I_0\equiv0$.

There is a tunneling effect in electron emission therefore we are trying also to fit our experimental data by the equation $I=I_0+(A+C\cdot E_{surf}^2)\cdot exp(-B/E_{surf})$ which is similar to Fowler-Nordheim (FN) equation.

In our experiments the laser pulse launch phase (φ) was scanned. The electric field at the cathode is $E_{surf}=E_{peak}\cdot sin(\varphi)$. The experimental data is presented in Fig.7. The data shows a good correlation to the FN like equation with $I_0=0$ and $C=0$:

ISBN 978-3-95450-115-1

Copyright © 2012 by IEEE – cc Creative Commons Attribution 3.0 (CC BY 3.0) — cc Creative Commons Attribution 3.0 (CC BY 3.0)

$$I(\varphi) = \frac{1}{\sigma\sqrt{2\pi}}\int exp\left(-\frac{(\theta-\varphi)^2}{2\sigma^2}\right)\Phi(\theta-F)A\cdot exp\left(-\frac{B}{E_{peak}\sin(\theta-F)}\right)d\theta \quad (1)$$

where φ is the launch phase, σ is the laser pulse rms width in radians; $\Phi(\theta\text{-}F)$ is Heaviside step function; *A*, *B* and *F* are fitted parameters of the FN like function.

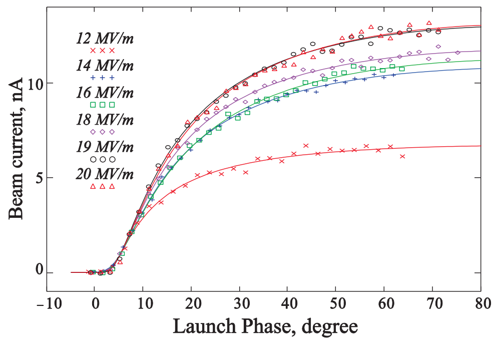

Figure 7: Photo current experimental data fitted by FN like equations.

To the raw data at each E_{peak} the dark current value at this field is subtracted (Fig.7). To the scanning phase a certain value (*F*) found by fitting is added to compensate the time dependent tuning of the phase drift between the scans. In Eq. 1 the Gaussian temporal distribution of the laser is taken into account by data convolution with the laser pulse.

We have to note, that the scan for one of the cavity field E_{peak} was made during a short time of about 10 min. But each scan was separated in time such that the first one (E_{peak}=12 *MV/m*) was made on the first day of the experiment and the other ones were made during the second day. Between these scans other experiments were carried out. This is one of the reasons for the variation in fitted coefficients *A* and *B* presented in Fig.8. The high power processing and laser cleaning of the cathode surface were going on during the separation time and these can cause the parameter growth.

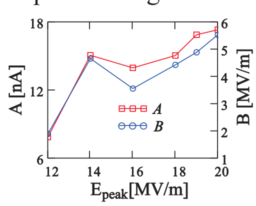

Figure 8: Parameters of the FN like fitting.

In Fig.9 all scanning data is brought together as a dependency on the cathode surface electric field (E_{surf}). The *12 MV/m* scan is excluded from this data due to its obvious irregularity. Also all initial data with launch phases of *0÷3* degrees (partially filled) are excluded. The fitting is made by the E_{surf} dependent FN like equation:

$$I(E_{surf}) = (A + C\cdot E_{surf}^2)\cdot exp\left(-\frac{B}{E_{surf}}\right). \quad (2)$$

In Eq.2 the small parameter *C* with square field factor typical for FN equation is defined here precisely due to the high number of data points (5 times more than each scan). Fitting parameters are following: *A=14.24 [nA], B=4.12 [MV/m], C=4.94·10*$^{-3}$ *[nA·MV*$^{-2}$*m*^{2}*]*.

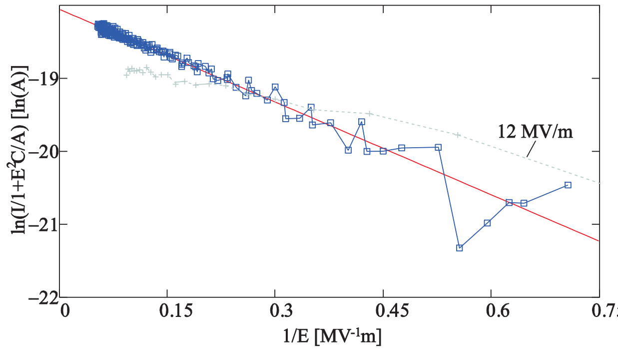

Figure 9: All experimental data with the FN like fitting. The convolution data with the laser pulse are excluded.

The simple physical explanation of such a fitting by Eq.2 can be as follows: some laser light is unable to produce electron emission (because I_0*=0,* probably work function is too large). Due to the laser light the work function of FN equation is reduced for laser activated electrons and new FN with $A\neq0$ becomes possible. Due to this the FN current of these activated electrons is only possible.

The reduced work function can be found from the exponent argument of the regular FN equation.

$$B = \frac{6830\phi^{1.5}}{\beta}, \quad (3)$$

where ϕ is the work function, β is the field enhancement factor. Solving Eq.3 for β=1,10,100 gives $\phi = 7.2\cdot10^{-3}, 0.033, 0.154$ eV respectively.

A perfect Schottky fitting is impossible here (see Fig.10).

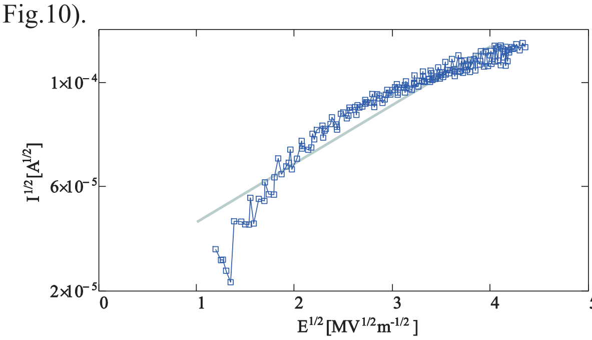

Figure 10: Schottky fitting of the data.

ACKNOWLEDGMENTS

The authors gratefully acknowledge Terry Atkinson for his fruit discussions for the work.

REFERENCES

[1] T. Kamps et all, IPAC 2011, San Sebastian, Spain, 2011.
[2] K.J. Kim, Nucl. Instr. And Meth. In Phis. Res. A275 (1989)
[3] K. Floettmann , TESLA-FEL Report 1997-01.
[4] J. Voelker et al., Proc. of IPAC 2012.
[5] Schottky W 1914 *Physik Z.* **15** 872.

Copyright © 2012 by IEEE – cc Creative Commons Attribution 3.0 (CC BY 3.0) — cc Creative Commons Attribution 3.0 (CC BY 3.0)